第二百二十八號

（昭和拾七年四月發行）

抄　錄

高速用對稱翼型の設計

囑託　岡本哲史
毛利浩

飛行機の高速化に伴ひ翼の摩擦抗力を減少せしめる事及び造波失速を遲らす事が問題になつて來た．翼の摩擦抗力を減少せしめるためには根本策として翼表面の境界層を出來るだけ層流に保つ事が望ましく，遷移が壓力上昇勾配に關係する事を考へれば翼表面に沿ふ壓力上昇勾配を出來るだけ緩かにする事が必要になる．このためには翼の最大厚位置を從來のものより幾分後退せしめねばならぬ．斯くすれば翼表面の最低壓力を高める事にもなるから，この事は造波失速の見地から見ても好都合の事である．かかる種類の翼型は既に我國でも設計されてゐるが，これらは凡て厚さ分布を多項式で表はしてゐる．この論文ではやり方を變へて厚さ分布即ち對稱翼型を吹出しと吸込みの組合せに依つて求めて見た．その結果これ迄にあまり得られてゐない樣な，壓力分布が翼の大部分で平坦になる樣な翼型を得る事が出來た．

No. 228.

(Published April, 1942.)

Design of Symmetrical Aerofoil Sections Suitable for High Speeds.

By

Tetusi OKAMOTO,

Research Associate of the Institute,

and

Hirosi MÔRI.

Abstract.

In order to reduce the frictional drag of the aerofoil it is desirable that the flow in the boundary layer retains laminar as possible along the surface. As the increasing pressure gradient is a cause of early transition from laminar to turbulent flow, it is necessary to make small the increasing pressure gradient along the surface. For this purpose the point of the maximum thickness of the aerofoil section must be shifted suitably backward. In the present paper the symmetrical aerofoil sections of such kinds were designed by the method of sources and sinks and the aerofoils with nearly uniform pressure distribution were obtained.

Introduction.

It is an important subject in improving the speed of aeroplane to reduce the air resistance of the parts of the aeroplane. As a method of reducing the frictional drag of the aerofoil it has been considered that the flow in the boundary layer retains laminar as possible along the surface. Although there are many unknown matters in the phenomena of the transition from laminar to turbulent flow, it is a well-known fact that the increasing pressure gradient is an important cause to hasten the transition. Consequently, it is desirable in designing the aerofoil sections suitable for high speeds to make small the rising pressure gradient and, if possible, to retain the pressure uniform along the surface. In order to shift backward the point of the lowest pressure, it is necessary to bring suitably backward the point of the maximum thickness of the aerofoil section, and this seems also favorable when considered from the point of view of delaying the occurrence of the compressibility burble to the highest speed as possible (Reference 1). The aerofoil sections of this kind have been designed by TANI and MITUISI (Reference 2) and FUKATSU (Reference 3) by using the method by which the N.A.C.A. aerofoils were designed (Reference 4). In this method the thickness distributions or the symmetrical aerofoils were expressed by the polynomials. In the present paper a group of the symmetrical aerofoil sections were designed by method of combining sources and sinks (Reference 5).

Flows due to sources.

In order to find the contours of the aerofoil section, the point source and the line sources having three types of strength distribution, namely, the uniform, the linear and the parabolic, were combined. We will now consider the potential flows due to sources.

(i) *Point source.* Suppose that a point source of strength m exists at the origin. Then, the potential function of the flow due to the source is

$$w = \frac{m}{2\pi} \log z \,, \qquad \ldots\ldots\ldots\ldots\ldots\ldots \quad (1)$$

where $z = x+iy$. Writing $C = \frac{m}{2\pi}$, the velocity potential φ_0 and the stream function ψ_0 are

$$\frac{\varphi_0}{C} = \log (x^2+y^2)^{\frac{1}{2}} \,, \qquad \ldots\ldots\ldots\ldots\ldots\ldots \quad (2a)$$

$$\left.\begin{aligned} \frac{\psi_0}{C} &= \tan^{-1}\frac{y}{x} - \pi \qquad \text{for} \quad x < 0 \,, \\ \frac{\psi_0}{C} &= \tan^{-1}\frac{y}{x} \qquad\quad \text{for} \quad x > 0 \,. \end{aligned}\right\} \ldots\ldots \quad (2b)$$

(ii) *Line source of uniformly distributed strength.* Suppose that the sources are distributed uniformly along the length l. Let m be the total strength. Then, the strength of the elementary strip $d\xi$ is $m\frac{d\xi}{l}$. Hence, the velocity potential and the stream function of the elementary source are from *Eq.* (1)

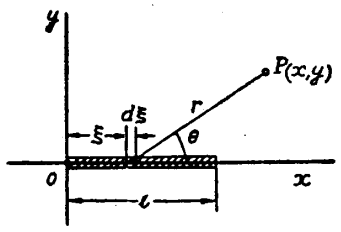

Fig. 1.

$$d\varphi_1 = \frac{m}{2\pi}\cdot\frac{d\xi}{l}\log r = \frac{Cd\xi}{2l}\log\left\{(x-\xi)^2+y^2\right\} \,,$$

$$d\psi_1 = \frac{m}{2\pi}\cdot\frac{d\xi}{l}\theta = \frac{Cd\xi}{l}\left(\tan^{-1}\frac{y}{x-\xi} - n\pi\right) \,,$$

where $C = \frac{m}{2\pi}$, $n = 1$ if $x < \xi$ and $n = 0$ if $x > \xi$. Integrating these,

$$\frac{\varphi_1}{C} = \frac{1}{2l}\int_0^l \log\left\{(x-\xi)^2+y^2\right\} d\xi \,, \qquad \ldots\ldots\ldots\ldots\ldots\ldots \quad (3a)$$

$$\frac{\psi_1}{C}=\frac{1}{l}\int_0^l \tan^{-1}\frac{y}{x-\xi}d\xi-L,$$

$$=\frac{1}{l}\left[x\tan^{-1}\frac{y}{x}-(x-l)\tan^{-1}\frac{y}{x-l}+\frac{y}{2}\log\frac{x^2+y^2}{(x-l^2)+y^2}\right]-L, \quad \cdots\cdots\cdots\cdots\cdots\cdots\cdots\cdots\cdots\cdots \quad (3b)$$

where $L=\pi$ if $x>0$, $L=\pi\left(1-\frac{x}{l}\right)$ if $0<x<l$ and $L=0$ if $l<x$.

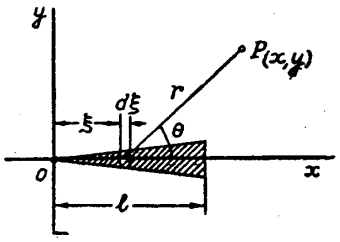

Fig. 2.

(iii) *Line source whose strength increases linearly along the line.* Let m be the total strength of the line source distributed along the length l. Then, the strength of the elementary strip $d\xi$ is $m\frac{2\xi d\xi}{l^2}$. Hence, the velocity potential and the stream function of the elementary source are from Eq. (1)

$$d\varphi_2=\frac{m}{2\pi}\cdot\frac{2\xi d\xi}{l^2}\log r=\frac{C\xi d\xi}{l^2}\log\{(x-\xi)^2+y^2\},$$

$$d\psi_2=\frac{m}{2\pi}\cdot\frac{2\xi d\xi}{l^2}\theta=\frac{2C\xi d\xi}{l^2}\left(\tan^{-1}\frac{y}{x-\xi}-n\pi\right),$$

where $n=1$ if $x<\xi$ and $n=0$ if $x>\xi$. Integrating these,

$$\frac{\varphi_2}{C}=\frac{1}{l^2}\int_0^l \log\left\{(x-\xi)^2+y^2\right\}\xi d\xi, \quad \cdots\cdots\cdots\cdots\cdots\cdots \quad (4a)$$

$$\frac{\psi_2}{C}=\frac{2}{l^2}\int_0^l \tan^{-1}\frac{y}{x-\xi}\xi d\xi-M,$$

$$=\frac{1}{l^2}\left[(x^2-y^2)\tan^{-1}\frac{y}{x}-(x^2-y^2-l^2)\tan^{-1}\frac{y}{x-l}-ly+xy\log\frac{x^2+y^2}{(x-l)^2+y^2}\right]-M, \quad \cdots\cdots \quad (4b)$$

where $M=\pi$ if $x<0$, $M=\pi\left(1-\frac{x^2}{l^2}\right)$ if $0<x<l$ and $M=0$ if $l<x$.

(iv) *Line source whose strength increases parabolically along the line.* Let m be the total strength of the line sources distributed along the length l. Then, the strength of the elementary strip $d\xi$ is $m\frac{3\xi^2 d\xi}{l^3}$. Hence, the velocity potential and the stream function of the elementary strip are

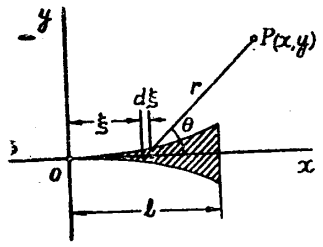

Fig. 3.

$$d\varphi_3=\frac{m}{2\pi}\cdot\frac{3\xi^2 d\xi}{l^3}\log r=\frac{3C\xi^2 d\xi}{2l^3}\log\left\{(x-\xi)^2+y^2\right\},$$

$$d\psi_3=\frac{m}{2\pi}\cdot\frac{3\xi^2 d\xi}{l^3}\theta=\frac{3C\xi^2 d\xi}{l^3}\left(\tan^{-1}\frac{y}{x-\xi}-n\pi\right),$$

where $n=1$ if $x<\xi$ and $n=0$ if $x>\xi$. Integrating these,

$$\frac{\varphi_3}{C}=\frac{3}{2l^3}\int_0^l\log\left\{(x-\xi)^2+y^2\right\}\xi^2 d\xi, \quad \cdots\cdots\cdots\cdots \quad (5a)$$

$$\frac{\psi_3}{C}=\frac{3}{l^3}\int_0^l\tan^{-1}\frac{y}{x-\xi}\xi^2 d\xi-N,$$

$$=\frac{1}{l^3}\left[-3x^2 I_1+3xI_2-(x-l)^3\tan^{-1}\frac{y}{x-l}+x^3\tan^{-1}\frac{y}{x}\right.$$

$$\left.-\frac{yl}{2}(l-2x)-\frac{y^3}{2}\log\frac{x^2+y^2}{(x-l)^2+y^2}\right]-N, \quad \cdots \quad (5b)$$

where $N=\pi$ if $x<0$, $N=\pi\left(1-\frac{x^3}{l^3}\right)$ if $0<x<l$ and $N=0$ if $l<x$. I_1 and I_2 denote the bracketed terms in the equations (3b) and (4b), respectively.

Determination of the contours of the aerofoil sections.

The velocity potential and the stream function of the parallel flow of velocity U are

$$\varphi_p = Ux\,, \qquad \psi_p = Uy \quad \ldots\ldots\ldots\ldots\ldots \quad (6)$$

Superimposing this parallel flow on the flows due to sources, the velocity potential and the stream function become

$$\frac{\varphi}{C} = \frac{\varphi_p}{C} + \sum \frac{\varphi_i}{C} = \frac{U}{C}x + \sum \frac{\varphi_i}{C}\,, \quad \ldots\ldots\ldots \quad (7a)$$

$$\frac{\psi}{C} = \frac{\psi_p}{C} + \sum \frac{\psi_i}{C} = \frac{U}{C}y + \sum \frac{\psi_i}{C}\,. \quad \ldots\ldots\ldots \quad (7b)$$

This combined flow of the parallel flow with the flows due to sources gives a boundary curve, which is, in general, not a closed curve. It becomes a closed curve, however, if the sinks are taken in the system of sources and the total sum of strength is made equal to zero.

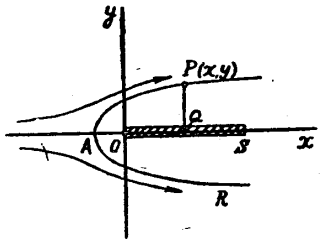

Fig. 4.

Suppose that the sources and sinks are suitably distributed along the line OS, and let the curve PAR be the boundary curve due to the combined flow of the parallel flow with the flows due to sources and sinks. Then, the stream function at any point $P(x, y)$ on the boundary curve is from Eq. (7b)

$$\psi = Uy + \sum \psi_i\,.$$

The value of ψ is the quantity of fluid passing through the line PQ, and the fluid cannot pass across the boundary curve. It follows that the value of ψ must be equal to the quantity of fluid appearing from the line OQ. Let this quantity be $\sum Q_i$. Then

$$Uy + \sum \psi_i = \sum Q_i\,.$$

Putting $\psi_i - Q_i = \psi_i'$, the above equation becomes

$$\frac{U}{C}y+\sum\frac{\psi_i'}{C}=0, \quad \cdots\cdots\cdots\cdots \quad (8)$$

which is the equation of the boundary curve. If the values of $-\sum\frac{\psi_i'}{C}$ are plotted against y for various values of x, then the boundary curve is graphically determined by the intersection of the lines of $\frac{U}{C}y$ with the curves of $-\sum\frac{\psi_i'}{C}$.

The coordinates of the leading edge are determined from the condition that the velocity at this point is zero, namely,

$$u=\frac{\partial}{\partial x}(Ux+\sum\varphi_i)=0$$

or
$$\frac{U}{C}=-\sum\frac{\partial}{\partial x}\left(\frac{\varphi_i}{C}\right)_{y=0}=-\sum\left(\frac{u_i}{C}\right)_{y=0}. \quad \cdots\cdots \quad (9)$$

Therefore, the coordinates of the leading edge can be found graphically from the curves of $-\sum\left(\frac{u_i}{C}\right)_{y=0}$ plotted against x. The values of $\left(\frac{u_i}{C}\right)_{y=0}$ are as follows:

for a point source

$$\left(\frac{\varphi_0}{C}\right)_{y=0}=\log x, \qquad \left(\frac{u_0}{C}\right)_{y=0}=\frac{1}{x}, \quad \cdots\cdots\cdots \quad (10)$$

for a line source of uniformly distributed strength

$$\left(\frac{\varphi_1}{C}\right)_{y=0}=\frac{1}{l}\int_0^l\log(x-\xi)d\xi$$
$$=\frac{1}{l}\left[(l-x)\log(x-l)+x\log x-l\right],$$
$$\left(\frac{u_1}{C}\right)_{y=0}=\frac{1}{l}\log\frac{x}{x-l}, \quad \cdots\cdots\cdots\cdots\cdots\cdots \quad (11)$$

for a line source whose strength increases linearly along the line

$$\left(\frac{\varphi_2}{C}\right)_{y=0}=\frac{2}{l^2}\int_0^l\xi\log(x-\xi)d\xi$$
$$=\frac{1}{l^2}\left[(l^2-x^2)\log(x-l)+x^2\log x-lx-\frac{l^2}{2}\right],$$

$$\left(\frac{u_2}{C}\right)_{y=0} = \frac{2}{l^2}\left(x \log \frac{x}{x-l} - l\right), \quad \cdots\cdots\cdots\cdots \quad (12)$$

and for a line source whose strength increases parabolically along the line

$$\left(\frac{\varphi_3}{C}\right)_{y=0} = \frac{3}{l^3}\int_0^l \xi^2 \log(x-\xi)d\xi$$

$$= \frac{1}{l^3}\left[(l^3-x^3)\log(x-l) + x^3 \log x - lx^2 - \frac{l^2x}{2} - \frac{l^3}{3}\right],$$

$$\left(\frac{u_3}{C}\right)_{y=0} = \frac{3}{l^3}\left(x^2 \log \frac{x}{x-l} - xl - \frac{l^2}{2}\right). \quad \cdots\cdots\cdots \quad (13)$$

The contours of the aerofoil sections calculated and the corresponding combinations of sources and sinks are shown in Fig. 5, and the ordinates of the contours of the aerofoil sections are tabulated in Table 1.

TABLE 1 (a). Ordinates for Aerofoil Sections.

(Stations and ordinates in percent of aerofoil chord.)

Station	K.D. 1	K.D. 2	K.D. 3	K.D. 4	K.D. 5	K.D. 6	K.D. 7	K.D. 8	K.D. 9	K.D. 10
0	0	0	0	0	0	0	0	0	0	0
0·5	—	—	—	—	1·53	1·27	0·95	0·85	0·68	1·60
1·25	1·88	1·04	0·51	0·26	2·48	1·98	1·46	1·24	0·97	2·45
2·5	2·92	1·75	0·91	0·49	3·48	2·68	1·92	1·61	1·27	3·38
5·0	4·49	2·82	1·57	0·88	4·72	3·58	2·49	2·06	1·61	4·60
7·5	5·70	3·66	2·12	1·21	5·60	4·23	2·91	2·39	1·85	5·49
10	6·70	4·37	2·59	1·48	6·30	4·74	3·25	2·66	2·05	6·23
15	8·27	5·51	3·34	1·94	7·36	5·53	3·79	3·09	2·38	7·43
20	9·49	6·39	3·91	2·28	8·19	6·14	4·21	3·43	2·64	8·38
30	11·10	7·53	4·63	2·71	9·29	6·95	4·75	3·87	2·98	9·61
40	11·88	8·09	4·98	2·93	9·81	7·33	4·99	4·07	3·13	10·09
50	11·99	8·18	5·02	2·96	9·83	7·33	4·99	4·07	3·13	9·88
60	11·50	7·83	4·78	2·81	9·35	6·95	4·72	3·84	2·97	9·00
70	10·37	7·00	4·23	2·47	8·29	6·10	4·11	3·32	2·56	7·48
80	8·44	5·60	3·33	1·92	6·54	4·73	3·13	2·51	1·92	5·40
90	5·49	3·49	2·00	1·12	3·95	2·80	1·79	1·42	1·07	2·87
95	3·36	2·04	1·11	0·61	2·25	1·58	0·98	0·78	0·58	1·48
100	0	0	0	0	0	0	0	0	0	0

TABLE I (b). Ordinates for Aerofoil Sections.

Station	K.D. 11	K.D. 12	K.D. 13	K.D. 14	K.D. 15	K.D. 16	K.D. 17	K.D. 18	K.D. 19	K.D. 20
0	0	0	0	0	0	0	0	0	0	0
0·5	1·26	0·89	0·64	1·67	1·42	1·12	0·74	1·86	1·43	1·24
1·25	1·88	1·28	0·88	2·58	2·09	1·57	1·01	2·90	2·29	1·88
2·5	2·54	1·68	1·11	3·61	2·84	2·06	1·29	3·99	3·12	2·50
5·0	3·35	2·18	1·41	4·82	3·79	2·67	1·65	5·31	4·10	3·16
7·5	3·96	2·56	1·66	5·68	4·46	3·12	1·91	6·14	4·70	3·60
10	4·48	2·89	1·88	6·37	4·99	3·48	2·12	6·80	5·17	3·94
15	5·36	3·45	2·25	7·46	5·82	4·04	2·45	7·80	5·88	4·46
20	6·06	3·90	2·54	8·29	6·45	4·48	2·71	8·55	6·41	4·84
30	6·97	4·49	2·91	9·32	7·24	5·03	3·03	9·52	7·08	5·32
40	7·31	4·70	3·03	9·69	7·51	5·20	3·13	9·98	7·40	5·54
50	7·10	4·54	2·92	9·45	7·28	5·01	3·00	9·99	7·41	5·55
60	6·38	4·03	2·59	8·58	6·54	4·46	2·64	9·56	7·07	5·28
70	5·19	3·22	2·07	7·11	5·33	3·58	2·09	8·58	6·30	4·68
80	3·63	2·20	1·39	5·14	3·78	2·49	1·43	6·93	5·02	3·69
90	1·85	1·09	0·68	2·74	1·97	1·26	0·72	4·43	3·08	2·23
95	0·93	0·54	0·33	1·41	1·00	0·63	0·36	2·70	1·76	1·27
100	0	0	0	0	0	0	0	0	0	0

TABLE I (c). Ordinates for Aerofoil Sections.

Station	K.D. 21	K.D. 22	K.D. 23	K.D. 24	K.D. 25	K.D. 26	K.D. 27	K.D. 28	K.D. 29	K.D. 30
0	0	0	0	0	0	0	0	0	0	0
0·5	1·85	1·49	1·20	1·10	0·87	0·57	0·36	—	—	—
1·25	2·86	2·32	1·84	1·65	1·24	0·81	0·50	0·32	0·20	0·10
2·5	3·94	3·16	2·48	2·27	1·62	1·07	0·63	0·62	0·39	0·20
5·0	5·28	4·18	3·18	3·07	2·17	1·41	0·82	1·18	0·73	0·38
7·5	6·20	4·85	3·65	3·73	2·64	1·71	0·99	1·71	1·06	0·57
10	6·91	5·36	4·01	4·32	3·08	1·99	1·15	2·22	1·39	0·75
15	8·00	6·16	4·59	5·38	3·89	2·51	1·45	3·18	2·03	1·12
20	8·82	6·77	5·03	6·34	4·63	2·99	1·73	4·06	2·63	1·48
30	9·82	7·54	5·57	7·99	5·91	3·84	2·24	5·56	3·67	2·13
40	10·15	7·77	5·71	9·20	6·88	4·51	2·67	6·67	4·48	2·63
50	9·84	7·48	5·47	9·86	7·43	4·91	2·93	7·30	4·96	2·92
60	8·92	6·70	4·87	9·87	7·45	4·94	2·96	7·33	5·00	2·95
70	7·41	5·48	3·94	9·10	6·85	4·54	2·72	6·72	4·58	2·69
80	5·39	3·90	2·76	7·49	5·58	3·67	2·17	5·44	3·68	2·14
90	2·94	2·05	1·42	4·94	3·60	2·30	1·30	3·48	2·27	1·29
95	1·54	1·05	0·72	3·16	2·18	1·35	0·72	2·14	1·34	0·73
100	0	0	0	0	0	0	0	0	0	0

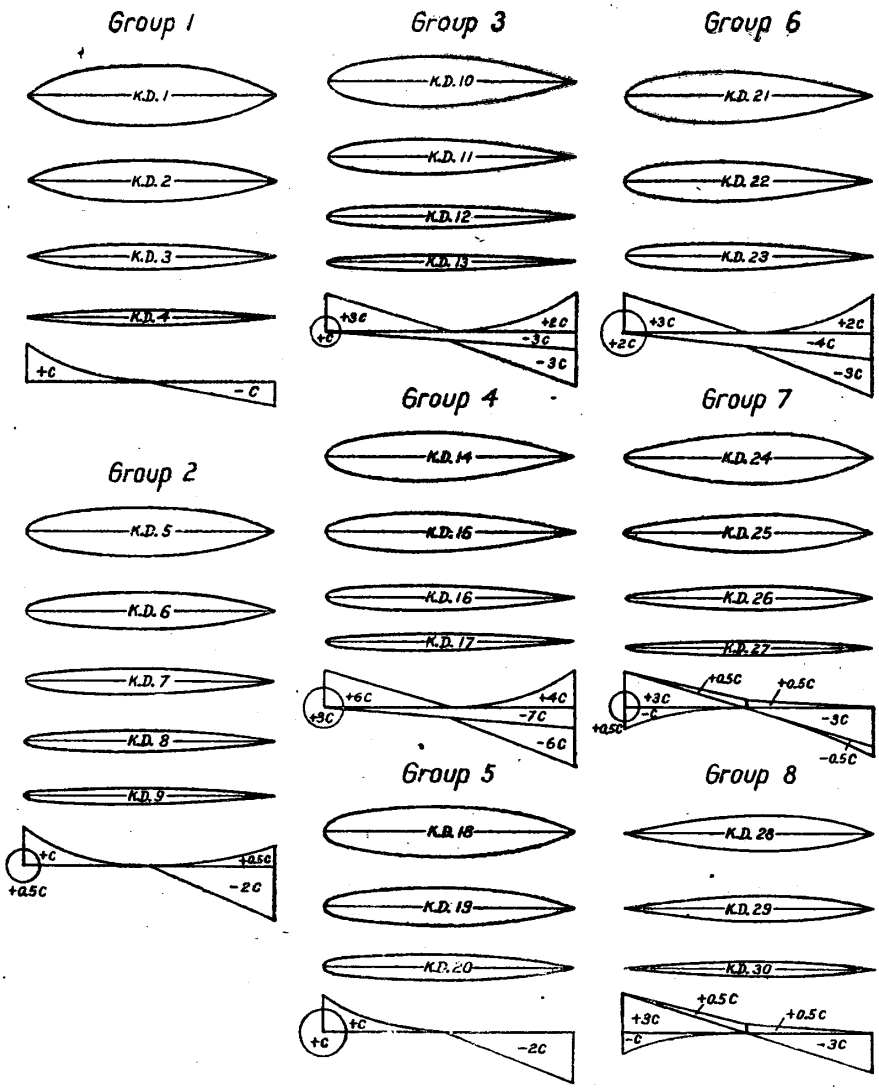

Fig. 5. The contours of the aerofoil sections and the corresponding distributions of sources and sinks.

Calculation of the pressure distribution.

The pressure distribution along the surface of the aerofoil section for zero angle of incidence is from BERNOULLI's equation

$$\frac{p-p_0}{\frac{1}{2}\rho U^2} = 1-\left(\frac{q}{U}\right)^2, \quad \cdots\cdots\cdots\cdots \quad (14)$$

where p_0, U are the pressure and the velocity of the undisturbed flow, p, q the pressure and the velocity on the surface of the aerofoil, and

$$q^2 = u^2+v^2 = (U+\sum u_i)^2+(\sum v_i)^2 . \quad \cdots\cdots\cdots \quad (15)$$

The values of u_i and v_i are as follows:
for a point source

$$\frac{u_0}{C} = \frac{\partial \varphi_0}{C\partial x} = \frac{x}{x^2+y^2} , \quad \cdots\cdots\cdots\cdots \quad (16a)$$

$$\frac{v_0}{C} = \frac{\partial \varphi_0}{C\partial y} = \frac{y}{x^2+y^2} , \quad \cdots\cdots\cdots\cdots \quad (16b)$$

for a line source of uniformly distributed strength

$$\frac{u_1}{C} = \frac{\partial \varphi_1}{C\partial x} = \frac{1}{2l}\int_0^l \frac{2(x-\xi)}{(x-\xi)^2+y^2}d\xi = \frac{1}{2l}\log\frac{x^2+y^2}{(x-l)^2+y^2}, \quad (17a)$$

$$\frac{v_1}{C} = \frac{\partial \varphi_1}{C\partial y} = \frac{1}{2l}\int_0^l \frac{2y}{(x-\xi)^2+y^2}d\xi = \frac{1}{l}\left[\tan^{-1}\frac{y}{x-l}-\tan^{-1}\frac{y}{x}+n\pi\right],$$

$$\cdots\cdots\cdots\cdots \quad (17b)$$

where $n = 1$ if $0<x<l$ and $n = 0$ if $x<0$ or $l<x$,
for a line source whose strength increases linearly along the line

$$\frac{u_2}{C} = \frac{\partial \varphi_2}{C\partial x} = \frac{1}{l^2}\int_0^l \frac{2(x-\xi)\xi}{(x-\xi)^2+y^2}d\xi = 2\left[\frac{x}{l}\cdot\frac{u_1}{C}+\frac{y}{l}\cdot\frac{v_1}{C}-\frac{1}{l}\right], \quad (18a)$$

$$\frac{v_2}{C} = \frac{\partial \varphi_2}{C\partial y} = \frac{1}{l^2}\int_0^l \frac{2y\xi}{(x-\xi)^2+y^2}d\xi = 2\left[\frac{x}{l}\cdot\frac{v_1}{C}-\frac{y}{l}\cdot\frac{u_1}{C}\right], \quad (18b)$$

and for a line source whose strength increases parabolically along the line

$$\frac{u_3}{C}=\frac{\partial\varphi_3}{C\partial x}=\frac{3}{2l^3}\int_0^l\frac{2(x-\xi)\xi^2}{(x-\xi)^2+y^2}d\xi$$

$$=3\left[\left(\frac{x^2}{l^2}-\frac{y^2}{l^2}\right)\frac{u_1}{C}+\frac{xy}{l^2}\cdot\frac{v_1}{C}-\frac{x}{l^2}-\frac{1}{2l}\right], \quad (19a)$$

$$\frac{v_3}{C}=\frac{\partial\varphi^3}{C\partial y}=\frac{3}{2l^3}\int_0^l\frac{2y\xi^2}{(x-\xi)^2+y^2}d\xi$$

$$=3\left[\left(\frac{x^2}{l^2}-\frac{y^2}{l^2}\right)\frac{v_1}{C}-2\frac{xy}{l^2}\cdot\frac{u_1}{C}+\frac{y}{l^2}\right]. \quad \ldots\ (19b)$$

The pressure distributions calculated are shown in Fig. 6 and tabulated in Table 2.

TABLE 2(a). Values of $\frac{p-p_0}{\frac{1}{2}\rho U^2}$.

(Stations in percent of aerofoil chord.)

Station	K.D. 1	K.D. 2	K.D. 3	K.D. 4	K.D. 5	K.D. 6	K.D. 7	K.D. 8	K.D. 9	K.D. 10
0	1·000	1·000	1·000	1·000	1·000	1·000	1·000	1·000	1·000	1·000
0·5	—	—	—	—	0·420	0·410	−0·070	−0·120	−0·175	0·530
1·25	0·530	0·520	0·520	0·530	−0·030	−0·089	−0·158	−0·142	−0·170	0·162
2·5	0·235	0·240	0·250	0·296	−0·134	−0·178	−0·180	−0·152	−0·144	−0·094
5·0	−0·057	−0·017	0·006	0·011	−0·283	−0·255	−0·198	−0·160	−0·126	−0·270
7·5	−0·196	−0·128	−0·093	−0·046	−0·348	−0·290	−0·205	−0·172	−0·130	−0·330
10	−0·295	−0·205	−0·140	−0·080	−0·384	−0·304	−0·213	−0·178	−0·136	−0·366
15	−0·439	−0·317	−0·196	−0·115	−0·423	−0·320	−0·220	−0·182	−0·140	−0·420
20	−0·522	−0·360	−0·222	−0·130	−0·440	−0·332	−0·222	−0·188	−0·142	−0·466
30	−0·583	−0·396	−0·243	−0·140	−0·458	−0·338	−0·230	−0·186	−0·139	−0·532
40	−0·591	−0·397	−0·239	−0·137	−0·465	−0·339	−0·230	−0·180	−0·137	−0·553
50	−0·588	−0·395	−0·237	−0·136	−0·468	−0·342	−0·232	−0·186	−0·142	−0·520
60	−0·571	−0·388	−0·237	−0·138	−0·465	−0·336	−0·231	−0·190	−0·142	−0·421
70	−0·518	−0·350	−0·210	−0·120	−0·408	−0·284	−0·200	−0·160	−0·120	−0·312
80	−0·392	−0·260	−0·155	−0·082	−0·277	−0·194	−0·126	−0·112	−0·077	−0·150
90	−0·142	−0·075	−0·036	−0·028	−0·026	−0·019	+0·005	−0·020	−0·005	+0·082
95	+0·077	+0·086	+0·069	+0·046	+0·204	+0·160	0·108	+0·092	+0·065	0·325
100	1·000	1·000	1·000	1·000	1·000	1·000	1·000	1·000	1·000	1·000

TABLE 2(b). Values of $\frac{p-p_0}{\frac{1}{2}\rho U^2}$.

Station	K.D. 11	K.D. 12	K.D. 13	K.D. 14	K.D. 15	K.D. 16	K.D. 17	K.D. 18	K.D. 19	K.D. 20
0	1·000	1·000	1·000	1·000	1·000	1·000	1·000	1·000	1·000	1·000
0·5	0·360	−0·062	−0·120	0·450	0·18[illegible]	−0·120	−0·183	0·360	0·560	0·010
1·25	−0·072	−0·119	−0·122	0·115	−0·138	−0·178	0·180	0·032	−0·080	−0·180
2·5	−0·178	−0·144	−0·110	−0·160	−0·276	−0·226	−0·163	−0·202	−0·317	−0·256
5·0	−0·240	−0·159	−0·100	−0·332	−0·323	−0·250	−0·147	−0·384	−0·386	−0·306
7·5	−0·259	−0·168	−0·102	−0·378	−0·327	−0·246	−0·134	−0·448	−0·383	−0·305
10	−0·274	−0·178	−0·112	−0·398	−0·330	−0·242	−0·126	−0·464	−0·374	−0·291
15	−0·303	−0·194	−0·120	−0·435	−0·339	−0·234	−0·134	−0·466	−0·354	−0·270
20	−0·338	−0·213	−0·134	−0·465	−0·361	−0·240	−0·140	−0·461	−0·339	−0·258
30	−0·380	−0·242	−0·153	−0·503	−0·392	−0·263	−0·158	−0·460	−0·326	−0·246
40	−0·400	−0·254	−0·161	−0·512	−0·400	−0·264	−0·162	−0·452	−0·324	−0·241
50	−0·373	−0·235	−0·150	−0·484	−0·367	−0·248	−0·142	−0·450	−0·325	−0·243
60	−0·312	−0·192	−0·120	−0·406	−0·308	−0·206	−0·113	0·454	−0·335	−0·245
70	−0·206	−0·126	−0·074	−0·288	−0·207	−0·133	−0·072	−0·416	−0·300	−0·224
80	−0·088	−0·044	−0·024	−0·132	−0·094	−0·060	−0·021	−0·320	−0·223	−0·163
90	+0·072	+0·068	+0·046	+0·053	+0·061	+0·031	+0·042	−0·095	−0·078	−0·039
95	0·171	0·158	0·102	0·206	0·199	0·118	0·075	+0·160	+0·224	+0·100
100	1·000	1·000	1·000	1·000	1·000	1·000	1·000	1·000	1·000	1·000

TABLE 2(c). Values of $\frac{p-p_0}{\frac{1}{2}\rho U^2}$.

Station	R.D. 21	K.D. 22	K.D. 23	R.D. 24	K.D. 25	K.D. 26	K.D. 27	K.D. 28	K.D. 29	K.D. 30
0	1·000	1·000	1·000	1·000	1·000	1·000	1·000	1·000	1·000	1·000
0·5	0·740	0·460	0·260	0·130	−0·002	−0·116	−0·190	—	—	—
1·25	0·320	−0·118	−0·242	0·065	−0·020	−0·108	−0·104	0·440	0·380	0·220
2·5	−0·198	−0·284	−0·311	0·001	−0·020	−0·047	−0·038	0·260	0·200	0·116
5·0	−0·412	−0·380	−0·332	−0·054	−0·041	−0 022	−0·019	0·141	0·103	0·064
7·5	−0·451	−0·394	−0·315	−0·082	−0·057	−0·034	−0·019	0·083	0·068	0·042
10	−0·468	−0·380	−0·293	−0·105	−0·068	−0·043	−0·020	0·038	0·035	0·025
15	−0·492	−0·375	−0·278	−0·182	−0·107	−0·065	−0·032	−0·056	−0·029	−0·013
20	−0·506	−0·380	−0·280	−0·220	−0·151	−0·091	−0·050	−0·121	−0·075	−0·042
30	−0·530	−0·402	−0·294	−0·333	−0·239	−0·156	−0·088	−0·242	−0·158	−0·096
40	−0·532	−0·403	−0·296	−0·442	−0·318	−0·205	−0·122	−0·330	−0·220	−0·127
50	−0·497	−0·375	−0·272	−0·520	−0·380	−0·247	−0·146	−0·397	−0·268	−0·157
60	−0·420	−0·310	−0·220	−0·540	−0·404	−0·265	−0·156	−0·419	−0·287	−0·168
70	−0·299	−0·208	−0·152	−0·518	−0·387	−0·252	−0·150	−0·388	−0·273	−0·158
80	−0·143	−0·096	−0·061	−0·434	−0·316	−0·197	−0·120	−0·310	−0·200	−0·120
90	+0·040	+0·036	+0·055	−0·217	−0·140	−0·064	−0·041	−0·122	−0·083	−0·038
95	0·210	+0·162	0·127	+0·153	+0·045	+0·052	+0·032	+0·047	+0·048	+0·036
100	1·000	1·000	1·000	1·000	1·000	1·000	1·000	1·000	1·000	1·000

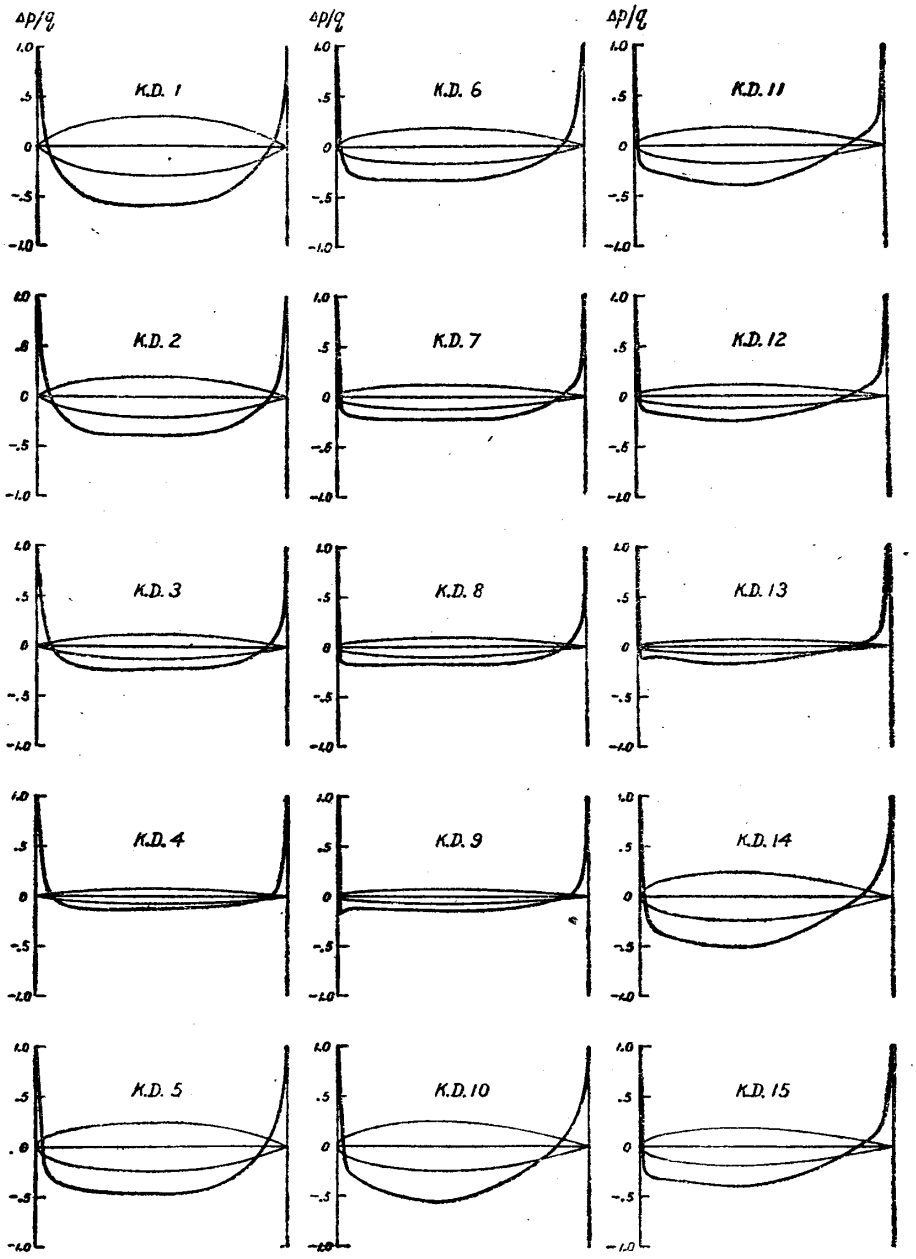

Fig. 6 (a). The calculated pressure distributions for zero angle of incidence.

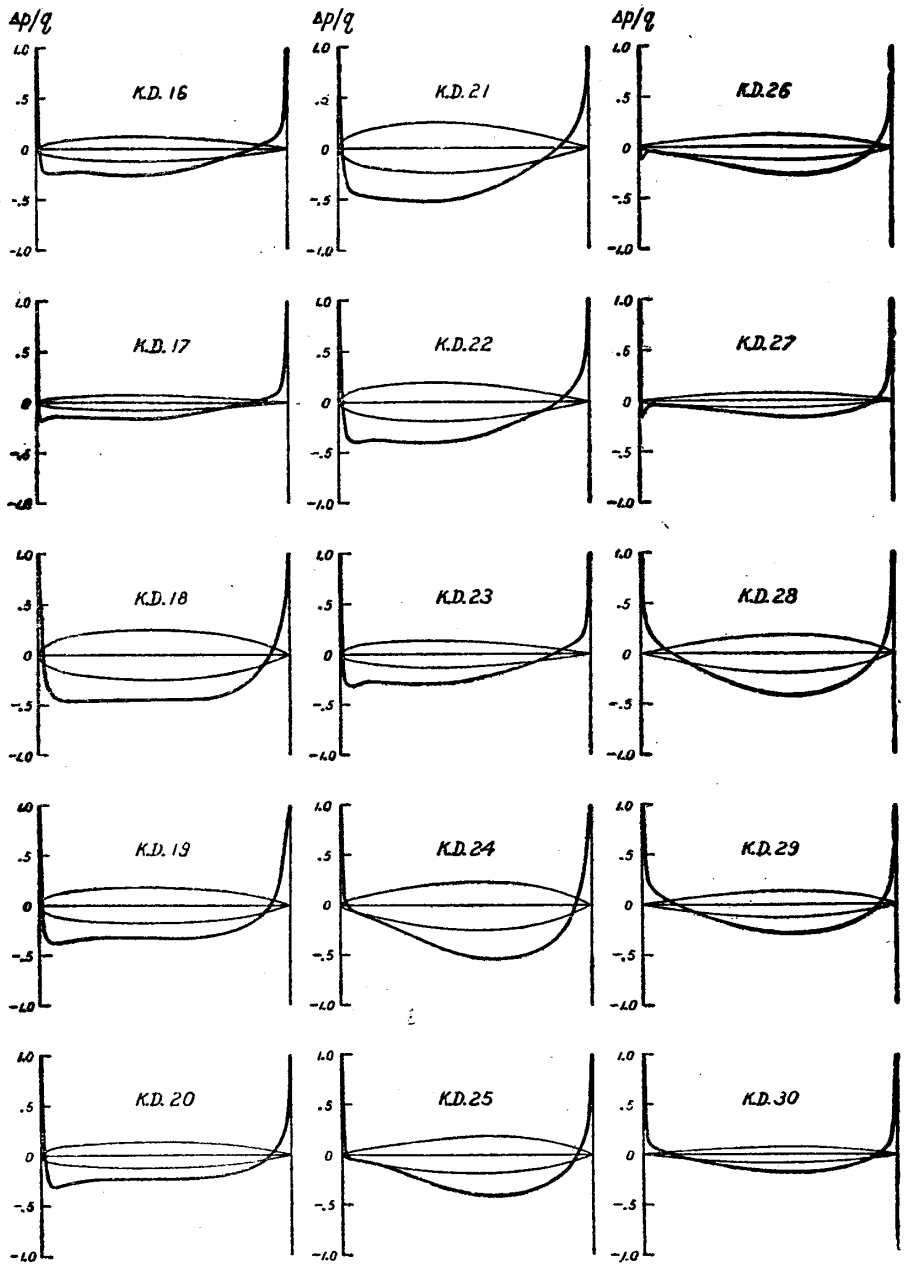

Fig. 6 (b).

Conclusions.

The symmetrical aerofoil sections whose pressure distributions are satisfactorily uniform over the large portions of the surface were theoretically obtained. The radius of leading edge increases with increasing the strength of the point source located at the nose. These aerofoil sections may be used as the thickness distribution in designing the cambered aerofoil section.

Research fund given by the Nippon Gakudyutu Sinkokwai enabled the above work to be carried out, for which the authors express their appreciation.

Aerodynamics Institute,
Tokyo University of Engineering,
January, 1942.

References.

1. J. STACK and A.E. von DOENHOFF ; Tests of 16 Related Airfoils at High Speeds. N.A.C.A. Tech. Rep. No. 492 (1934).
2. I. TANI and S. MITUISI ; Contributions to the Design of Aerofoils Suitable for High Speeds. Rep. Aero. Res. Inst., Tokyo Imp. Univ. No. 198 (1940 .
3. R. FUKATSU ; A Method of Designing the Aerofoil Sections by Combining Aerofoils (in Japanese). Jour. Aero. Res. Inst., Tokyo Imp. Univ. No. 204 (1941).
4. E.N. JACOBS, K.E. WARD and R.M. PINKERTON ; The Characteristics of 78 Related Airfoil Sections from Tests in the Variable-Density Wind Tunnel. N.A.C.A. Tech. Rep. No. 460 (1933).
5. A. FUHRMANN ; Theoretische und Experimentalle Untersuchungen an Balloonmodellen : Jahrbuch der Motorluftschiff-Studien-Gesellschaft, Bd. V. (1911–12).

TH. v. KÁRMÁN ; Berechnung der Druckverteilung an Luftschiffkörpern. Abhand.. Aero. Inst., Techn. Hochs. Aachen, Heft 6 (1927).

S. AGAWA ; On the Strut Forms. Jour. Aere. Res. Inst., Tokyo Imp. Univ. No. 31 (1927).

R.H. SMITH ; Aerodynamic Theory and Tests of Strut Forms, Part II. N.A.C.A. Tech. Rep. No. 335 (1929).